Volume 16, Issue 4, 162532 (1-11)

International Journal of Nano Dimension (IJND)

https://dx.doi.org/10.57647/j.ijnd.2025.1604.32

# DFT assessments on a Chitosan-modified nanocone scaffold for the adsorption of ciclopirox antifungal drug to provide insights into the engineering a potential nano-based drug delivery platform

Chou-Yi Hsu[1,2,*], Radhwan Abdul Kareem[3], Oybek Ruziyev[4], Afet Mastan Jafarova[5], Mahmoud Mirzaei[6,*]

[1]*Thunderbird School of Global Management, Arizona State University, Tempe Campus, Phoenix, Arizona 85004, USA.*
[2]*Department of Pharmacy, Chia Nan University of Pharmacy and Science, Tainan 71710, Taiwan.*
[3]*Ahl Al Bayt University, Karbala, Iraq.*
[4]*Department of Medical Fundamental Sciences, Termez University of Economics and Service, Termez, Uzbekistan.*
[5]*Department of Engineering and Applied Sciences, Azerbaijan State University of Economics (UNEC), Baku, Azerbaijan.*
[6]*Department of Natural and Mathematical Sciences, Faculty of Engineering, Tarsus University, Tarsus, Türkiye.*

[*]**Corresponding authors:** chouyihs@asu.edu, mahmoudmirzaei@tarsus.edu.tr

**Original Research**

Received:
30 March 2025
Revised:
20 May 2025
Accepted:
25 May 2025
Published online:
26 May 2025
Published in issue:
1 June 2025



**Abstract:**

This work was done by the benefit of employing density functional theory (DFT) calculations for assessing a chitosan-modified nanocone scaffold (S) for the adsorption of ciclopirox antifungal drug (D) to provide insights into the engineering a potential nano-based drug delivery platform by the formation of DS complexes. Two scaffolds were prepared; S1 and S2, and three complexes were obtained for each scaffold by the adsorption of D substance yielding DS11, DS12, and DS13 for S1 and DS21, DS22, and DS23 for S2. The strength of DS2 complexes were found higher than DS1 complexes, in which DS11 and DS21 were the strongest ones in each category. Regarding the evaluation of electronic features, small changes were found for the frontier molecular orbital levels of models and their related features. As a result, formations of DS complexes were found suitable for approaching the main goal of this work by obtaining suitable strengths for the complex systems. Hence, the existence of non-covalent interactions between the adsorbate and adsorbent counterparts and obtaining remarkable electronic features actually approved the applicability of employing S1 and S2 for adsorbing the specific D substance for investigating further developments of nano-based delivery of ciclopirox antifungal drug.

**Keywords:** Adsorption; Computational assessment; Drug interaction; Nanomedicine; Nanostructure

## 1. Introduction

Regarding the critical issues in dealing with health sciences, developing novel drug delivery platforms has been a crucial step for approaching a controllable level of targeted medical treatment of diseases with a higher efficiency in comparison with the conventional treatments [1, 2]. Assigning a suitable scaffold for the adsorption of drug substance could help to approach a successful complex formation of drug-carrier system to be handled for the drug delivery platform [3, 4]. To this aim, fabricating a carrier scaffold and examining its features has been targeted by several researchers for years to customize a carrier for a specific drug substance [5, 6]. However, the achieved successes have not been certain yet and many more investigations should be handled to overcome the complicated topic of drug treatments of diseases in an efficient way [7, 8]. Chitosan; as a biopolymer composed of glucosamine monomers, has been known to work as a possible carrier in the drug delivery systems, in which its combination with other substances such as nanostructures provided even more suitable scaffolds for interacting with the drug substances [9–11]. Indeed, several applications of

chitosan-based systems have been investigated up to now for working in the biological related media, in which the characteristic features should be still examined for approaching more suitable application of such system for desired biological purposes [12, 13]. Nanostructures themselves have been also introduced as characteristic materials for employing in several fields of applications with a significance of applications in the biological and health related media [14, 15]. The results of earlier works indicated that the modification of nanostructures or combining them with other substances could lead to obtain better results for the case of adsorbing other substances in comparison with the pure nanostructures [16, 17]. Additionally, different structural shapes and architectures of nanostructures were found as other characteristic issues of these systems for working in specific purposes and the modification could be known as an enhancement method of employing such featured materials [18, 19].
Nanocone is a typical conical architecture of nanostructure for involving in different applications with a suitability of adding functional groups to the tip-apex for generating complex systems [20, 21]. Within the current research work, the tip-apex of a representative nanocone was functionalized by a glucosamine monomer of chitosan biopolymer to prepare a modified scaffold for adsorbing the ciclopirox antifungal drug substance regarding the development of nano-based drug delivery platforms. As shown in figure 1, the glucosamine molecule was added to a nanocone within its two atomic sites of involving in chitosan biopolymer system along with the ether connection bridge. It is worth to remind here that the chitosan biopolymer is composed of glucosamine monomers, in which one monomer was used in this work to provide the material of a molecular scale study [22, 23]. Accordingly, S1 and S2 were designed as two modified scaffolds for involving in the adsorption of ciclopirox drug (D) substance (figure 2) to obtain the drug-scaffold (DS) complex systems as shown in figure 3. The models were prepared using the benefits of density functional theory (DFT) calculations to obtain the optimized systems and their characteristic features for engineering a potential nano-based drug delivery platform [24, 25]. To this aim, the molecular models were prepared using the optimization calculations and their features were evaluated in both of numerical and graphical representations as listed in Tables 1-3 and exhibited in figures 1-5. The main purpose of current work was focused on the recognition of a potential carrier along with the fabrications of a modified scaffold as a practical adsorbent of ciclopirox drug. Accordingly, details of interacting systems and their features before and after DS complex formations were evaluated to realize the efficiency of targeted systems to be engineered as a potential nano-based drug delivery platform. Structural and electronic characterizations were done accordingly to show benefits of employing the engineered platform of this work for further investigations of such complicated systems.
The term of antifungal is generally related to those medicines with killing or stopping roles against the growth of infectious fungi, which are also called as antimycotic agents [26]. Fungal and microbial infections have very serious negative impacts on the human health systems without any certain treatment against them [27, 28]. Ciclopirox is a common prescribed antifungal for medicating moderate onychomycosis of fingernails and toenails besides treating seborrheic dermatitis [29]. In a chemist's point of view, ciclopirox is a 2-hydroxypyridine derivative so called a hydroxypyridine antifungal agent [30]. By the importance of this antifungal agent, the drug delivery of ciclopirox was studied by earlier works to assess benefits of combinations of drug and carrier systems for approaching better results [31–34]. Indeed, a wide spectrum of prescription of ciclopirox made it as an important topic to be investigated for approaching more successes on its use for medication of fungal infections [35]. Accordingly, the current research work was carried out to make DFT assessments on a chitosan-modified nanocone scaffold (DS) for the adsorption of ciclopirox antifungal drug (D) to provide insights into the engineering a potential nano-based drug delivery platform along with the formation of drug-scaffold (DS) complexes.

## 2. Materials and methods

Within this research work, S1 and S2 models were prepared using the combination of a glucosamine molecule; as a monomer of chitosan biopolymer, and a nanocone along with different atomic sites of glucosamine for the forma-

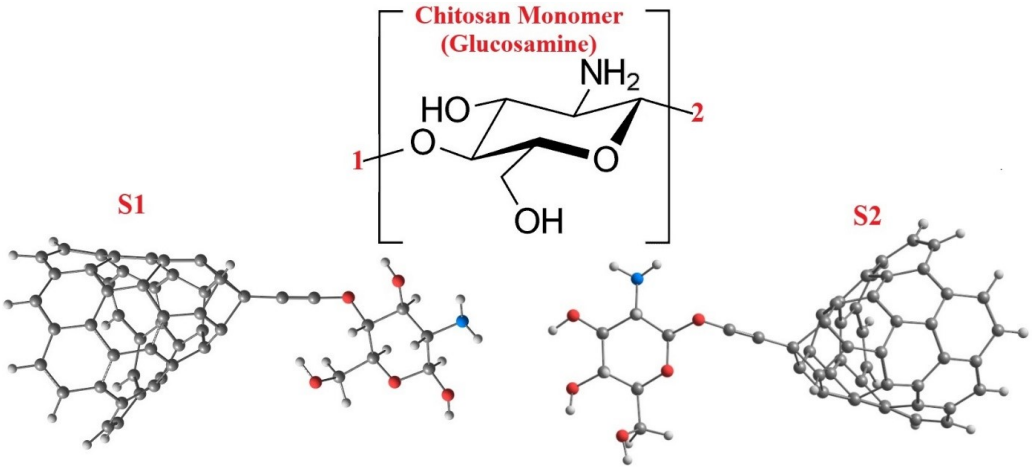


**Figure 1.** Chitosan-modified nanocone scaffolds (S1 and S2) composed from different atomic sites of chitosan monomer.

tion of chitosan biopolymer. The models were optimized to stabilize the S1 and S2 scaffolds to be examined as possible adsorbents of ciclopirox antifungal drug (D) (figure 2). Next, combinations of D with each of S1 and S2 scaffolds were examined by performing additional optimization calculations, in which three conformations were found for each scaffold as indicated by DS11, DS12, and DS13 for the combinations of D with S1, and DS21, DS22, and DS23 for the combinations of D with S2 (figure 3). All calculations of this work were done based on DFT for optimizing the molecular models and evaluating their features using the popular ωB97XD/6-31G* method/basis set as implemented in the Gaussian 16 program [36]. Strengths of adsorptions were evaluated for the complex systems as listed in Table 1 including the impact of counterpoise basis set superposition error (BSSE) [37]. Stabilities of models were confirmed by performing additional vibrational frequency calculations not to show the existence of any imaginary frequency. By obtaining the optimized systems, the involving interactions were identified by the quantum theory of atoms in molecule (QTAIM) and the non-covalent interaction (NCI) analyses using the Multiwfn 3.8 program [38] as represented in Table 2 and figures 3 and 4. Afterwards, the frontier molecular orbital based electronic features were evaluated using the Chemcraft 1.8 and gaussSum 3.0 programs [39, 40] regarding the energy values of the highest occupied molecular orbital (HOMO) and the lowest unoccupied molecular orbital (LUMO) levels as represented in Table 3 and figure 5. Indeed, the current research work was done by the benefits of employing computer-based tools to investigate the existence and featured properties of molecular models for developing their further functions and applications for desired purposes [41–44]. In this regard, the evaluated results of this work could be expected to reveal insights into the fabrication of an appropriate chitosan-modified nanocone scaffold (S) for adsorbing the ciclopirox antifungal drug (D) to be engineered in a potential nano-based drug delivery platform along with the formation of drug-scaffold (DS) complexes.

## 3. Results and discussion

To approach the idea of this work, two forms of a chitosan-modified nanocone scaffold; identified as S1 and S2, were assessed for the adsorption of ciclopirox antifungal drug (D) to provide insights into the engineering a potential nano-based drug delivery platform. Formations of DS complex systems regarding various modes of interactions were examined along with DFT calculations. Singular and complex models were prepared (figure 1-3) and their stabilities were found through the geometrical optimization calculations. Next, details of complex systems and electronic features were evaluated to approach the aim of this work. To assess details of investigated models, the evaluated features were discussed in the following domains.

### 3.1 Models preparation and adsorption strength

The main model of this work was the chitosan-modified nanocone scaffold, in which the way of attachment of chitosan monomer (glucosamine) to the apex-tip of nanocone yielded two scaffolds as shown by S1 and S2 in figure 1. As mentioned in the Introduction part, the glucosamine monomer was used as a representative of chitosan biopolymer in this molecular scale study. Both of S1 and S2 models were optimized in the single-standing state in addition to the optimization of single-standing ciclopirox antifungal drug as indicated by D (figure 2). Next, the models were

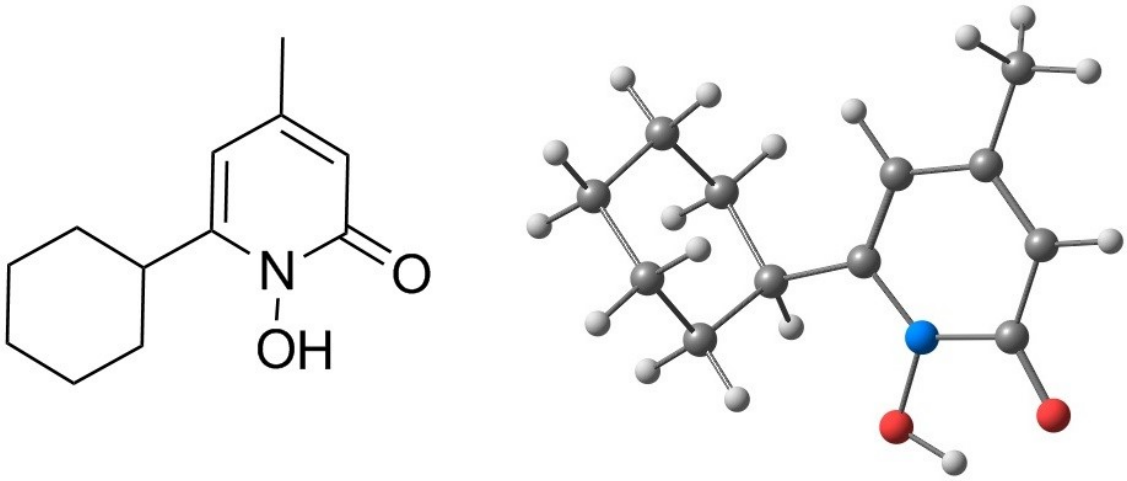


**Figure 2.** Ciclopirox drug (D).

**Table 1.** Adsorption energy ($E_{Ads}$ kcal/mol) of drug-scaffold complex systems (figure 3).*

| System | DS11 | DS12 | DS13 | DS21 | DS22 | DS23 |
|---|---|---|---|---|---|---|
| $E_{Ads}$ | −10.94 | −7.74 | −7.37 | −11.77 | −10.98 | −8.10 |

*$E_{Ads} = E_{DS} - E_S - E_D + BSSE$

combined to each other for the formation of interacting complexes including the D and each of S1 and S2 scaffolds, in which three models of complexes were found for each scaffold including DS11, DS12, and DS13 for the formation of D and S1 interactions and DS21, DS22, and DS23 for the formation of D and S2 interactions. The complex models were optimized and their finalized forms were shown in figure 3 to be assessed for the formation of drug-scaffold complexes. Within these models, the scaffold was assigned as the adsorbent and the drug was assigned as the adsorbate and the whole process was assigned as an adsorption process for the formation of adsorbate- adsorbent complexes. Accordingly, the term of adsorption strength was identified for these systems based on the energy differences of complexes and their counterparts. As listed in Table 1, the models were stabilized with different levels of strength as found by −10.94, −7.74, and −7.37 kcal/mol for the formation of DS11, DS12, and DS13 systems and −11.77, −10.98, and −8.10 kcal/mol for the formation of DS21, DS22, and DS23 systems. In this regard, the models were found in different modes of formations regarding different scaffolds and also the relaxation of D substance towards the scaffold. It is important to describe the achievement on the adsorption processes which show the significance of modes of interactions between the substances to yield the desired systems. Accordingly, the models were found in different levels of strength regarding their found values of $E_{Ads}$. DS11 and DS21 were found at the highest level of strength for each category of scaffolds showing the best relaxation way of D towards the S1 and S2 scaffolds, in which the S2 scaffold was found even at a higher level of strength in comparison with the S1 scaffold regarding the obtained values of $E_{Ads}$. As a conclusion, although all complex models were found strong enough to yield the formation of DS complexes, but the models related to the S2 scaffold yielded stronger adsorption processes than the models related to the S1 scaffold. As examined for the whole possible interacting geometries, these models were finalized based on their energy features and geometrical specifications. Hereby, DS11, DS12, DS13, DS21, DS22, and DS23 were assigned as the final complex models of this work. As a result, the models were involved in further investigations for learning their details and specifications.

### 3.2 QTAIM and NCI analyses

For identifying the involving interactions and describing their features, the complex models were assessed regarding the QTAIM and NCI analyses. The shown interaction in figure 3 for the complexes were found based on the QTAIM analysis and their corresponding features were summarized

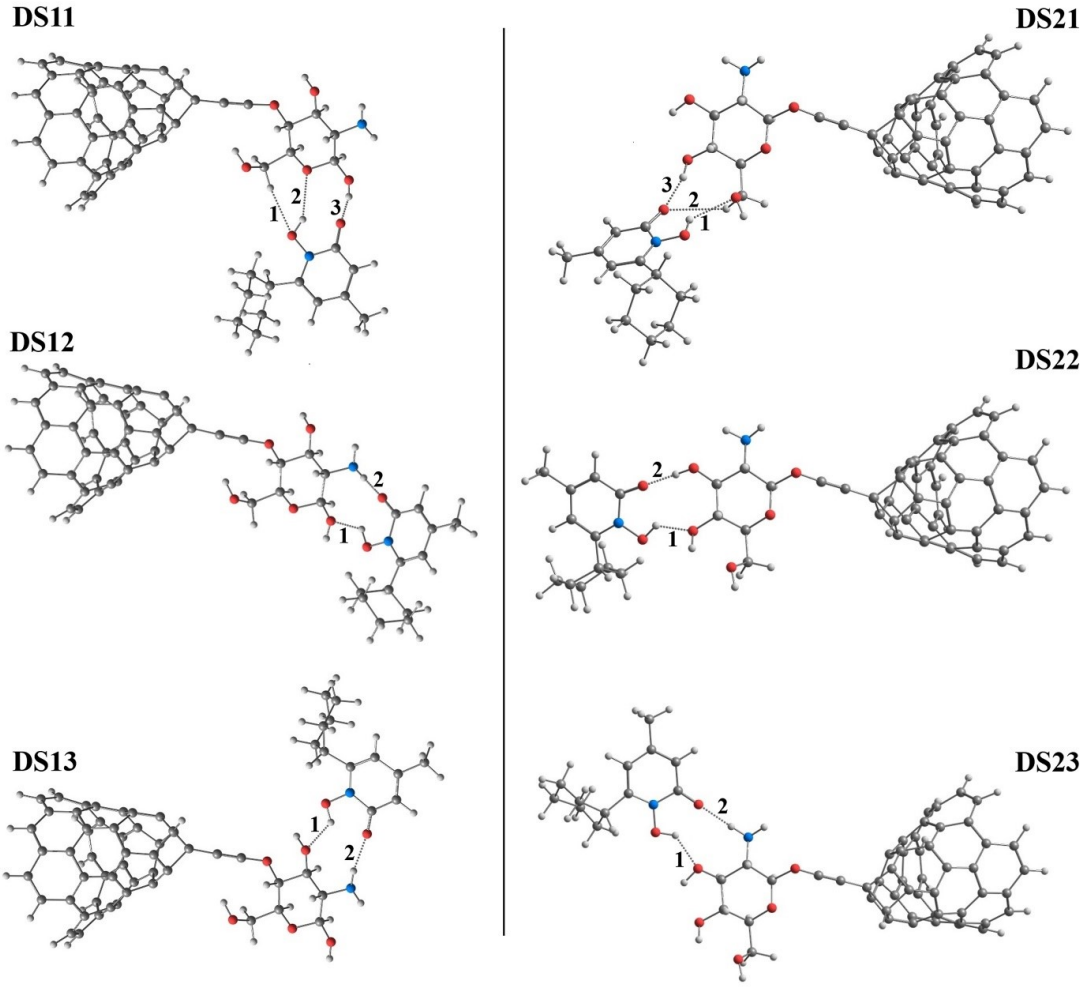


**Figure 3.** Drug-scaffold (DS) complex systems composed from varieties of interaction possibilities between drug (D) and each scaffold (S1 and S2).

**Table 2.** QTAIM features (in au) of interactions in drug-scaffold complex systems (figure 3).*

| System | Interaction | Distance (Å) | $\rho$ | $\nabla^2\rho$ | K(r) | V(r) | H(r) |
|---|---|---|---|---|---|---|---|
| DS11 | 1: O…H | 2.61 | 0.0059 | 0.0262 | −0.0013 | −0.0039 | 0.0013 |
| | 2: H…O | 2.73 | 0.0044 | 0.0204 | −0.0012 | −0.0027 | 0.0012 |
| | 3: O…H | 1.82 | 0.0325 | 0.1095 | 0.0004 | −0.0282 | −0.0004 |
| DS12 | 1: H…O | 2.01 | 0.0220 | 0.0763 | 0.0002 | −0.0196 | −0.0002 |
| | 2: O…H | 2.06 | 0.0188 | 0.0675 | −0.0005 | −0.0159 | 0.0005 |
| DS13 | 1: H…O | 2.09 | 0.0189 | 0.0649 | 0.0002 | −0.0167 | −0.0002 |
| | 2: O…H | 2.06 | 0.0185 | 0.0687 | −0.0006 | −0.0158 | 0.0006 |
| DS21 | 1: H…O | 2.38 | 0.0107 | 0.0383 | −0.0005 | −0.0086 | 0.0005 |
| | 2: O…H | 3.04 | 0.0032 | 0.0139 | −0.0008 | −0.0018 | 0.0008 |
| | 3: O…H | 1.86 | 0.0279 | 0.1034 | −0.0005 | −0.0248 | 0.0005 |
| DS22 | 1: H…O | 1.95 | 0.0249 | 0.0835 | 0.0006 | −0.0219 | −0.0006 |
| | 2: O…H | 1.81 | 0.0312 | 0.1185 | −0.0008 | −0.0279 | 0.0008 |
| DS23 | 1: H…O | 1.98 | 0.0236 | 0.0771 | 0.0007 | −0.0207 | −0.0007 |
| | 2: O…H | 1.98 | 0.0217 | 0.0801 | −0.0006 | −0.0188 | 0.0006 |

*These features were directly extracted from the calculation results.

in Table 2. Additionally, the results of NCI analysis were shown in figure 4. As shown in the complex systems, three interactions were found for the formation of DS11 and DS21 whereas the rest of models were found based on the involvement of two interactions in each complex model. As a result, formations of DS11 and DS21 complexes were at the strongest level for each category of S1 and S2 scaffolds comparing to other models of the same category. Comparing distances of interactions (Table 2) between D and S counterparts in two categories of S1 and S2 scaffolds indicated that the models of S2 related complexes were stabilized at shorter distances towards each other than the models of S1 related complexes. Accordingly, the adsorption strength was found differently for the complex models in each category. Moreover, the models were described regarding the electronic based energy features of each interaction at its bond critical point (BCP) in the complex using the evaluated QTAIM features; $\rho$, $^2\rho$, K(r), V(r), and H(r), implying for density of all electrons, Laplacian of electron density, Hamiltonian kinetic energy, potential energy density, and energy density. As a general issue, the signs of QTAIM features are very important for their recognition, as the negative sign for both of $^2\rho$ and H(r) stands for a covalent bond and the positive sign for both of $^2\rho$ and H(r) stands for an electrostatic bond. The interaction will be partially covalent in the case of negative sign of $^2\rho$ only and it will be a strong electrostatic interaction in the case of negative sign of H(r) only. Hereby, different modes of interactions could be seen for the involving interactions in each complex and in the comparative complexes. In this regard, the models were found to be available in the non-covalent interactions, which is a representative of pushing forward the reversible adsorption processes. Hence, an occurrence of desorption process could be expected for the obtained non-covalent complexes. In this case, the models were found suitable for working in the drug delivery process, as the loaded drug should be released from the carrier scaffold.

Additional assessments of interactions were done based on the results of noncovalent interaction (NCI) analysis as described in the plots of figure 4, scattered by the values of reduced density gradient (RDG) over the $\text{sign}(\lambda_2)\rho$ for each interaction. The left region of plot with negative values of $\text{sign}(\lambda_2)\rho$ implies for the existence of hydrogen bond or electrostatic interactions, the central region of plot with zero values of $\text{sign}(\lambda_2)\rho$ implies for the existence of van der Waals interactions, and the right region of plot with positive values of $\text{sign}(\lambda_2)\rho$ implies for the existence of strong repulsive interactions. As could be learned by the obtained results of NCI analysis, the existence of electrostatic nature of interaction was obvious for each involving interaction in the presence of normal repulsive terms. Accordingly, based on the results of QTAIM features and the complementary NCI scatter plots, the formation of complexes was related to the existence of meaningful interactions between the counterparts. Additionally, strong interactions were found for the formations of DS11 and DS21 approving the achievement on the formation of these two complexes. To this point, the models were found practical for approaching a reversible adsorption process making possible the occurrence of desorption also.

### 3.3 HOMO-LUMO related features

Regarding the achievements of structural analyses, the models of this study were found stable enough to be investigated

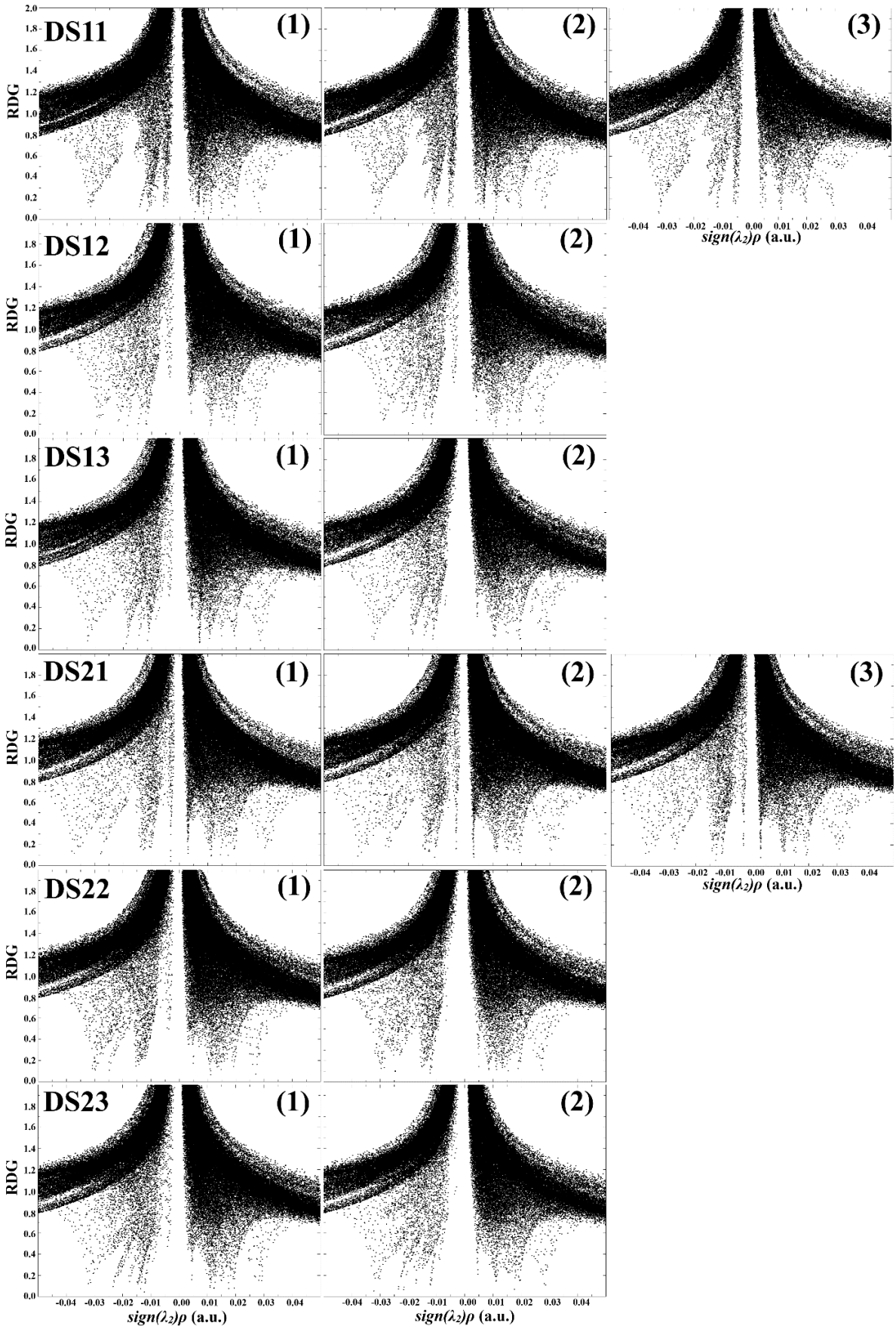


**Figure 4.** Non-covalent interaction (NCI) analyses of drug-scaffold (DS) complex systems for each represented interaction in figure 3 assigned by numbers in the parenthesis.

**Table 3.** Molecular orbital features (in eV) of singular scaffolds and drug systems and their drug-scaffold complex systems (Figures 1-3).*.

| System | $E_{HOMO}$ | $E_{LUMO}$ | $E_{Gap}$ | $\mu$ | $\eta$ | $\omega$ |
|---|---|---|---|---|---|---|
| D | −7.74 | 1.00 | 8.74 | −3.37 | 4.37 | 1.30 |
| S1 | −6.51 | −1.57 | 4.94 | −4.04 | 2.47 | 3.30 |
| S2 | −6.39 | −1.40 | 4.99 | −3.90 | 2.49 | 3.05 |
| DS11 | −6.48 | −1.52 | 4.95 | −4.00 | 2.48 | 3.23 |
| DS12 | −6.47 | −1.53 | 4.95 | −4.00 | 2.47 | 3.23 |
| DS13 | −6.49 | −1.54 | 4.94 | −4.01 | 2.47 | 3.26 |
| DS21 | −6.31 | −1.32 | 5.00 | −3.82 | 2.50 | 2.91 |
| DS22 | −6.34 | −1.34 | 5.00 | −3.84 | 2.50 | 2.95 |
| DS23 | −6.34 | −1.34 | 4.99 | −3.84 | 2.50 | 2.95 |

*Descriptions of evaluated features:
$E_{HOMO}$ (Energy of the highest occupied molecular orbital); directly extracted from the calculation results.
$E_{LUMO}$ (Energy of the lowest unoccupied molecular orbital); directly extracted from the calculation results.
$E_{Gap}$ (Energy of gap between HOMO and LUMO) = $E_{LUMO} - E_{HOMO}$
$\mu$ (Chemical potential) = $(E_{LUMO} + E_{HOMO})/2$
$\eta$ (Chemical hardness) = $(E_{LUMO} - E_{HOMO})/2$
$\omega$ (Electrophilicity index) = $(\mu)^2/(2\eta)$

for analyzing their electronic features. Accordingly, the HOMO-LUMO related features were evaluated for the investigated systems and they were listed in Table 3. Additionally, the visualized representations of distribution patterns and density of states (DOS) spectra were exhibited in figure 5. As could be found by the results, different values of $E_{HOMO}$ and $E_{LUMO}$ were observed for S1 and S2 scaffolds showing the changes of electronic features of models regarding the way of modification of nanocone using the glucosamine monomer of chitosan biopolymer. In this case, the values of $E_{Gap}$ showed also changes of features based on the variations of HOMO and LUMO levels. Indeed, these frontier levels are very important to be investigated for the electronic features of molecular models because of their significant roles for pushing forward the electronic transactions inside and outside of the molecule. To this point, the models of this work including the singular D, S1 and S2 and the complexes were investigated based on the HOMO-LUMO features. Comparing the values of $E_{Gap}$ for S1 and the corresponding DS11, DS12, and DS13 complexes and for S2 and the corresponding DS21, DS22, and DS23 complexes were found slightly different in each category. This achievement could be related to the stability of each modified scaffold to keep its initial electronic feature even by adsorbing the drug substance in the complex state. On the other hand, levels of HOMO and LUMO were changed for the systems from the singular scaffold to the corresponding complexes. The visualized DOS spectra also showed variations of those molecular orbital levels before and after the dominant HOMO and LUMO levels, in which monitoring such variations could be useful for approving the adsorption process of drug substance by the scaffold. Moreover, the values of $E_{Gap}$ and also variations of HOMO and LUMO levels could be observed directly by the visualized DOS spectra of molecular systems.

In addition to the discussed electronic features, other related features were listed in Table 3 standing for chemical potential ($\mu$), chemical hardness ($\eta$), and electrophilicity index ($\omega$). As could be found by the obtained results, the electronic features were changed regarding the changes of HOMO and LUMO levels yielding values of additional electronic features. Changes of value from the singular scaffold to the corresponding complex system could be followed by the evaluated information. Although slight changes were found among the models, but the way of scaffold modification and also the type of obtained complexes were important to achieve the results. In other words, the structural features have their significance on the electronic features and they could define the next applications and functions of molecular systems. As could be found for the investigated systems, all models of adsorption process could be expected suitable for the formations of complexes but their own specific features.

## 4. Conclusion

The main goal of this work was focused on the investigation of two forms of a chitosan-modified nanocone scaffold; S1 and S2, for the adsorption of ciclopirox antifungal drug (D) to provide insights into the engineering a potential nano-based drug delivery platform regarding the formation of DS complex systems along with DFT calculations. In this regard, the molecular models of singular and complex systems were characterized based on structural and electronic features. The achievements of this work could be summarized in some notations regarding their discussed content. The first notation could be considered on the way of modification of nanocone with the chitosan monomer, in which S2 was found stronger than S1 for adsorbing the drug substance by the formation of stronger DS2 complexes than DS1 complexes. In both systems,

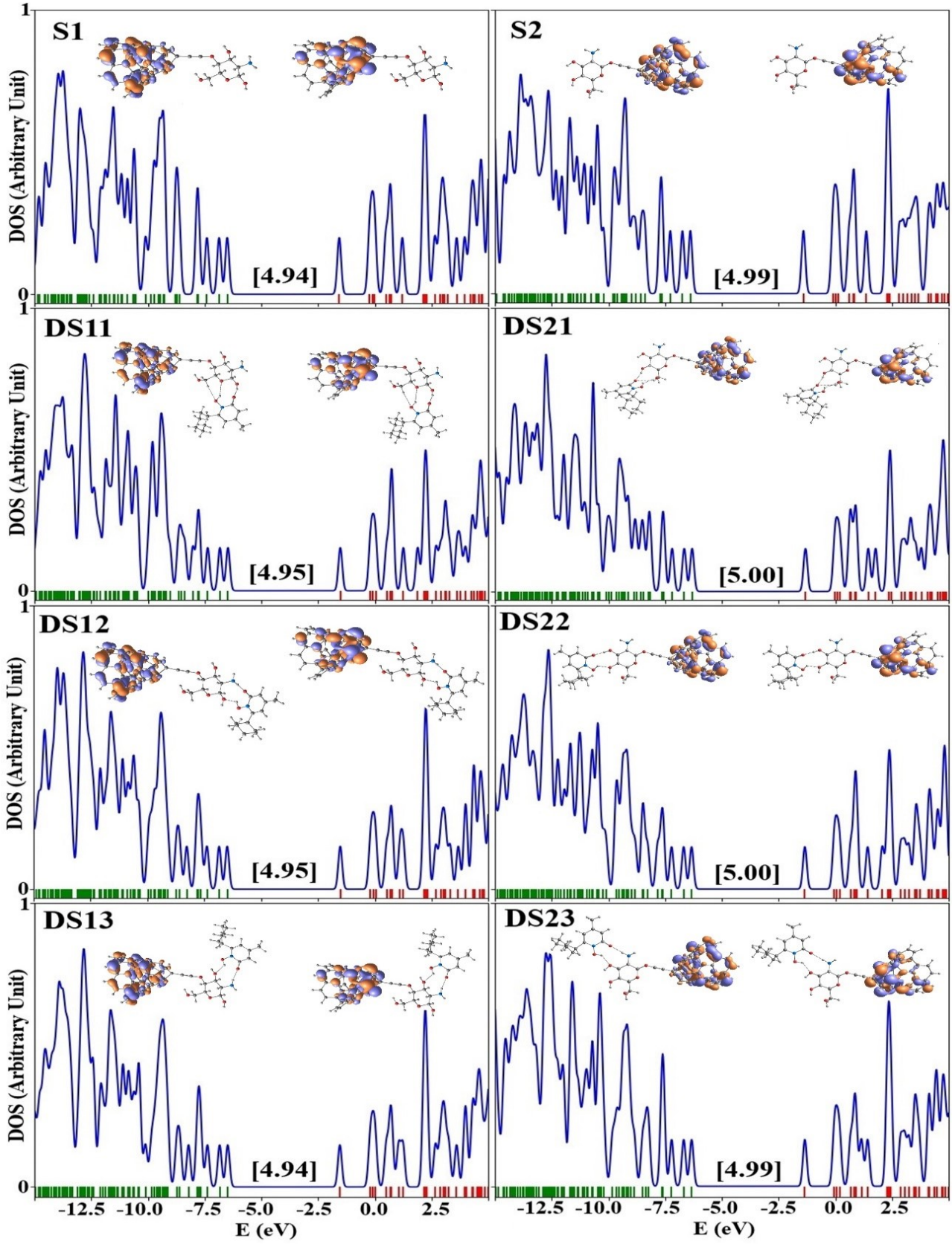


**Figure 5.** DOS spectra of singular scaffold (S1 and S2) systems and drug-scaffold (DS) complex systems including HOMO (left-green) and LUMO (right-red) distribution patterns in each panel.

one complex involving three interactions was the strongest model of complex formation. The second notation could be considered on the QTAIM features, in which the counterparts of DS2 complexes were relaxed closer to each other than the counterparts of DS1 complexes. Accordingly, features of each interaction were identified based on the evaluated features showing the existence of non-covalent interactions in the complex systems. These issues were re-checked by the results of NCI analysis for the complexes. The third notation could be considered on the electronic features of scaffolds, in which the main features were kept in the complex systems showing independency of complexes to the relaxation of conformations regarding the electronic variations. In this case, the complex models of each category were slightly different from each other, but the two categories were more different. And as a final notation, formations of DS11, DS12, and DS13 complexes for the adsorption of D by the assistance of S1 scaffold and formations of DS21, DS22, and DS23 complexes for the adsorption of D by the assistance of S2 scaffold were found suitable for approaching the main goal of this work. Obtaining suitable strengths for the complex systems along with the existence of non-covalent interactions between the adsorbate and adsorbent counterparts and obtaining remarkable electronic features actually approved the applicability of employing S1 and S2 for adsorbing the specific D substance for investigating further developments of nano-based delivery of ciclopirox antifungal drug.

**Authors contributions**
Authors have contributed equally in preparing and writing the manuscript.

**Availability of data and materials**
The authors declare that the data supporting the findings of this study are available within the paper.

**Conflict of interests**
The authors assert that they do not have any identifiable conflicting financial interests or personal relationships that might be perceived to influence the work presented in this paper.

## References


[1] M. T. Manzari, Y. Shamay, H. Kiguchi, N. Rosen, M. Scaltriti, and D. A. Heller. "Targeted drug delivery strategies for precision medicines.". *Nature Reviews Materials*, 6:351, 2021. DOI: https://doi.org/10.1038/s41578-020-00269-6.

[2] E. Veg, K. Hashmi, S. Raza, S. Joshi, A. Rahman Khan, and T. Khan. "The role of nanomaterials in diagnosis and targeted drug delivery.". *Chemistry & Biodiversity*, 22:e202401581, 2025. DOI: https://doi.org/10.1002/cbdv.202401581.

[3] P. Trucillo. "Drug carriers: classification, administration, release profiles, and industrial approach.". *Processes*, 9:470, 2021. DOI: https://doi.org/10.3390/pr9030470.

[4] Y. Li, W. Liu, Y. Wang, and S. Lu. "Cellulose based nano-scaffolds for targeted cancer therapies: Current status and future perspective.". *International Journal of Nanomedicine*, 20:199, 2025. DOI: https://doi.org/10.2147/IJN.S500261.

[5] M. K. Malik, P. Bhatt, T. Kumar, J. Singh, V. Kumar, A. Faruk, S. Fuloria, N. K. Fuloria, V. Subrimanyan, and S. Kumar. "Significance of chemically derivatized starch as drug carrier in developing novel drug delivery devices.". *Natural Products Journal*, 13:40, 2023. DOI: https://doi.org/10.2174/2210315512666220819112334.

[6] M. J. Saadh, C. Y. Hsu, R. A. Kareem, A. M. Jafarova, A. Zareii, M. Edalat, and M. Mirzaei. "Computational assessments of 5-Fluorocytosine (Flucytosine) antifungal adsorption onto a fullerene oxide nanocage for engineering a potential drug delivery platform.". *Chemical Review and Letters*, 8, 2025. DOI: https://doi.org/10.22034/crl.2025.512441.1561.

[7] S. Adepu and S. Ramakrishna. "Controlled drug delivery systems: Current status and future directions.". *Molecules*, 26:5905, 2021. DOI: https://doi.org/10.3390/molecules26195905.

[8] J. Pei, Y. Yan, C. P. Palanisamy, S. Jayaraman, P. M. Natarajan, V. R. Umapathy, S. Gopathy, J. R. Roy, J. C. Sadagopan, D. Thalamati, and M. Mironescu. "Materials-based drug delivery approaches: Recent advances and future perspectives.". *Green Processing and Synthesis*, 13:20230094, 2024. DOI: https://doi.org/10.1515/gps-2023-0094.

[9] G. Wang, R. Li, B. Parseh, and G. Du. "Prospects and challenges of anticancer agents' delivery via chitosan-based drug carriers to combat breast cancer: A review.". *Carbohydrate Polymers*, 268: 118192, 2021. DOI: https://doi.org/10.1016/j.carbpol.2021.118192.

[10] B. Tian, Y. Liu, and J. Liu. "Chitosan-based nanoscale and non-nanoscale delivery systems for anticancer drugs: A review. ". *European Polymer Journal*, 154:110533, 2021. DOI: https://doi.org/10.1016/j.eurpolymj.2021.110533.

[11] M. Saeedi, O. Vahidi, M. R. Moghbeli, S. Ahmadi, M. Asadnia, O. Akhavan, F. Seidi, M. Rabiee, M. R. Saeb, T. J. Webster, and R. S. Varma. "Customizing nano-chitosan for sustainable drug delivery.". *Journal of Controlled Release*, 350:175, 2022. DOI: https://doi.org/10.1016/j.jconrel.2022.07.038.

[12] P. Doroudgar, B. Mousavi-fard, M. Khadematolrasoul, F. Shams, E. Khashabi, and Z. Mirzae Gabaran. "Evaluation of the effect of chitosan and titanium dioxide nanoparticles mixed with orthodontic primer on shear bond strength: a systematic review and meta-analysis.". *International Journal of Scientific Research in Dental and Medical Sciences*, 6:184, 2024. DOI: https://doi.org/10.30485/ijsrdms.2024.489237.1618.

[13] F. Karam and S. Dakhel. "Bioactivity assessment of the prepared chitosan-based Schiff base composite on lung cancer and esophageal cancer.". *Chemical Review and Letters*, 7:816, 2024. DOI: https://doi.org/10.22034/crl.2024.462460.1359.

[14] S. Waheed, Z. Li, F. Zhang, A. Chiarini, U. Armato, and J. Wu. "Engineering nano-drug biointerface to overcome biological barriers toward precision drug delivery.". *Journal of Nanobiotechnology*, 20: 395, 2022. DOI: https://doi.org/10.1186/s12951-022-01605-4.

[15] S. Sabbagh Seddigh, A. Fazlzadeh, and S. Sabbagh Seddigh. "Evaluation of the diagnostic accuracy of carbon nanoparticle suspensions in sentinel lymph node biopsy of breast cancer: A systematic review and meta-analysis.". *International Journal of Scientific Research in Dental and Medical Sciences*, 5:154, 2023. DOI: https://doi.org/10.30485/ijsrdms.2023.414143.1529.

[16] M. Nezamabadi, E. Balali, and M. Qomi. "A sumanene-chitosan scaffold for the adsorption of niraparib anticancer: DFT insights into the drug delivery.". *Inorganic Chemistry Communications*, 155: 111098, 2023. DOI: https://doi.org/10.1016/j.inoche.2023.111098.

[17] S. A. Kakil, H. Y. Abdullah, and T. G. Abdullah. "The impact of lead on structural, electronic, and vibrational properties of pristine C36 and its boron, nitrogen-dopant C36 on pentagonal and hexagonal rings.". *Chemical Physics Impact.*, 7:100360, 2023. DOI: https://doi.org/10.1016/j.chphi.2023.100360.

[18] N. Osman, N. Devnarain, C. A. Omolo, V. Fasiku, Y. Jaglal, and T. Govender. "Surface modification of nano-drug delivery systems for enhancing antibiotic delivery and activity.". *Wiley Interdisciplinary Reviews: Nanomedicine and Nanobiotechnology*, 14:e1758, 2022. DOI: https://doi.org/10.1002/wnan.1758.

[19] M. Nasrollahzadeh, Z. Issaabadi, M. Sajjadi, S. M. Sajadi, and M. Atarod. "Types of nanostructures.". *Interface Science and Technology*, 28:29, 2019. DOI: https://doi.org/10.1016/B978-0-12-813586-0.00002-X.

[20] M. C. Shanmukha, A. Usha, K. C. Shilpa, and M. K. Siddiqui. "Structural investigation of carbon nanocone through topological coindices.". *International Journal of Quantum Chemistry*, 123: e27109, 2023. DOI: https://doi.org/10.1002/qua.27109.

[21] J. C. Charlier and G. M. Rignanese. "Electronic structure of carbon nanocones.". *Physical Review Letters*, 86:5970, 2001. DOI: https://doi.org/10.1103/PhysRevLett.86.5970.

[22] D. R. Smith, A. P. Escobar, M. N. Andris, B. M. Boardman, and G. M. Peters. "Understanding the molecular-level interactions of glucosamine-glycerol assemblies: a model system for chitosan plasticization.". *ACS Omega*, 6:25227, 2021. DOI: https://doi.org/10.1021/acsomega.1c03016.

[23] S. Jeremić, T. H. Tran, Z. Marković, T. C. Ngo, and D. Q. Dao. "Insight into interaction properties between mercury and lead cations with chitosan and chitin: Density functional theory studies.". *Computational and Theoretical Chemistry*, 1138:99, 2018. DOI: https://doi.org/10.1016/j.comptc.2018.06.010.

[24] G. A. Okon, D. G. Malu, H. Y. Abdullah, C. R. Nwokoye, N. I. Gber, C. P. Egbo, J. A. Unyime, and T. E. Gber. "Chalcogenides encapsulated Pt-doped carbon quantum dot (Pt@CQD) as a carrier for the controlled release of lapachone: outlook from theoretical calculations.". *Diamond and Related Materials*, 149:111628, 2024. DOI: https://doi.org/10.1016/j.diamond.2024.111628.

[25] I. Vaziri, I. Amini, M. R. Poor Heravi, and R. Rzayev. "A density functional theory study of adsorption dimethyl fumarate on the surface of the pristine of g-C3N4 and Fe, Ni and Cu decorated graphitic carbon nitride.". *Chemical Review and Letters*, 8:52, 2025. DOI: https://doi.org/10.22034/crl.2024.454286.1327.

[26] E. Sturabotti, A. Camilli, F. Leonelli, and F. Vetica. "Carbon dots as bioactive antifungal nanomaterials.". *ChemMedChem*, 19: e202400463, 2024. DOI: https://doi.org/10.1002/cmdc.202400463.

[27] S. Gnat, D. Łagowski, A. Nowakiewicz, and M. Dylag. "A global view on fungal infections in humans and animals: opportunistic infections and microsporidioses.". *Journal of Applied Microbiology*, 131:2095, 2021. DOI: https://doi.org/10.1111/jam.15032.

[28] S. Munipati, H. Rachamadugu, S. Avileli, R. Avula, N. J. Beladona, and S. R. Boyapally. "Microbiological profile of post-COVID-19 mucormycosis in various samples.". *International Journal of Scientific Research in Dental and Medical Sciences*, 4:87, 2022. DOI: https://doi.org/10.30485/ijsrdms.2022.338567.1285.

[29] E. Y. Gaballah, T. M. Borg, and E. A. Mohamed. "Hydroxypropyl chitosan nail lacquer of ciclopirox-PLGA nanocapsules for augmented *in vitro* nail plate absorption and onychomycosis treatment.". *Drug Delivery*, 29:3304, 2022. DOI: https://doi.org/10.1080/10717544.2022.2144543.

[30] J. Tao, H. Li, J. Zuo, Y. Li, F. Chen, and Y. Kang. "Development and scale-up of a fully continuous flow synthesis of 2-hydroxypyridine-N-oxide.". *Organic Process Research & Development*, 28:1640, 2023. DOI: https://doi.org/10.1021/acs.oprd.3c00285.

[31] S. Kaviani, S. Shahab, M. Sheikhi, V. Potkin, and H. Zhou. "A DFT study of Se-decorated B12N12 nanocluster as a possible drug delivery system for ciclopirox.". *Computational and Theoretical Chemistry*, 1201:113246, 2021. DOI: https://doi.org/10.1016/j.comptc.2021.113246.

[32] J. Kishishita, C. de Almeida Perez Pimenta, D. P. Cerqueira Macedo, M. B. Delgado-Charro, and L. Bastos Leal. "New formulation–microporation combination approaches to delivering ciclopirox across human nails.". *Pharmaceutics*, 16:72, 2024. DOI: https://doi.org/10.3390/pharmaceutics16010072.

[33] Z. Haleem Al-Qaim, M. Adil, A. J. Kadhim, R. Ali Abdalhuseen, H. Abdulhasan Hammoodi, A. S. Abed, M. Abosaooda, and H. Soleymanabadi. "The drug delivery of ciclopirox anticancer by γ-graphyne and its boron nitride analogue: electronic study via DFT.". *Molecular Physics*, 122:e2273980, 2024. DOI: https://doi.org/10.1080/00268976.2023.2273980.

[34] T. Ahmed, M. A. Rahman, R. Islam, A. A. Piya, and S. U. Shamim. "Unravelling the adsorption performance of BN, AlN, GaN and InN 2D nanosheets towards the ciclopirox, 5-fluorouracil and nitrosourea for anticancer drug delivery motive: A DFT-D with QTAIM, PCM and COSMO investigations.". *Computational and Theoretical Chemistry*, 1214:113797, 2022. DOI: https://doi.org/10.1016/j.comptc.2022.113797.

[35] P. Mucha, B. Borkowski, A. Erkiert-Polguj, and E. Budzisz. "Ciclopirox and ciclopirox olamine: antifungal agents in dermatology with expanding therapeutic potential.". *Applied Sciences*, 14:11859, 2024. DOI: https://doi.org/10.3390/app142411859.

[36] Gaussian 16, Revision C.01, M. J. Frisch, G. W. Trucks, H. B. Schlegel, G. E. Scuseria, M. A. Robb, J. R. Cheeseman, G. Scalmani, V. Barone, G. A. Petersson, H. Nakatsuji, X. Li, M. Caricato, A. V. Marenich, J. Bloino, B. G. Janesko, R. Gomperts, B. Mennucci, H. P. Hratchian, J. V. Ortiz, A. F. Izmaylov, J. L. Sonnenberg, D. Williams-Young, F. Ding, F. Lipparini, F. Egidi, J. Goings, B. Peng, A. Petrone, T. Henderson, D. Ranasinghe, V. G. Zakrzewski, J. Gao, N. Rega, G. Zheng, W. Liang, M. Hada, M. Ehara, K. Toyota, R. Fukuda, J. Hasegawa, M. Ishida, T. Nakajima, Y. Honda, O. Kitao, H. Nakai, T. Vreven, K. Throssell, J. A. Montgomery Jr., J. E. Peralta, F. Ogliaro, M. J. Bearpark, J. J. Heyd, E. N. Brothers, K. N. Kudin, V. N. Staroverov, T. A. Keith, R. Kobayashi, J. Normand, K. Raghavachari, A. P. Rendell, J. C. Burant, S. S. Iyengar, J. Tomasi, M. Cossi, J. M. Millam, M. Klene, C. Adamo, R. Cammi, J. W. Ochterski, R. L. Martin, K. Morokuma, O. Farkas, J. B. Foresman, and D. J. Fox. "Effect of temperature on properties of aluminum/single-walled carbon nanotube nanocomposite by molecular dynamics simulation.". *Proc Inst Mech Eng C: J Mech Eng Sci.*, 234:635–42, 2020. DOI: https://doi.org/10.1177/0954406219878760.

[37] A. Galano and J. R. Alvarez–Idaboy. "A new approach to counterpoise correction to BSSE.". *Journal of Computational Chemistry*, 27:1203, 2006. DOI: https://doi.org/10.1002/jcc.20438.

[38] T. Lu. "A comprehensive electron wavefunction analysis toolbox for chemists, Multiwfn.". *Journal of Chemical Physics*, 161:082503, 2024. DOI: https://doi.org/10.1063/5.0216272.

[39] Chemcraft-graphical software for visualization of quantum chemistry computations. Version 1.8, build 682. URL https://www.chemcraftprog.com.

[40] N. M. O'boyle, A. L. Tenderholt, and K. M. Langner. "Cclib: a library for package-independent computational chemistry algorithms.". *Journal of Computational Chemistry*, 29:839, 2008. DOI: https://doi.org/10.1002/jcc.20823.

[41] M. R. Sameti and M. Torkashvand. "Theoretical evaluation of C24 nanocage functionalization with protons for enhanced sulfacetamide drug delivery: a DFT study with non-covalent interaction analyses. ". *Journal of Molecular Structure*, 1318:139298, 2024. DOI: https://doi.org/10.1016/j.molstruc.2024.139298.

[42] R. Ahmadi, M. R. Jalali Sarvestani, and B. Sadeghi. "Computational study of the fullerene effects on the properties of 16 different drugs: A review.". *International Journal of Nano Dimension*, 9:325, 2018. URL https://ijnd.tonekabon.iau.ir/article_660200.html.

[43] R. Ghiasi, M. Nikbakht, and H. Pasdar. "Interactions of the potential antitumor agent vanadocene dichloride with C20 and M+@ C20 (M=Li, Na, K) nano-cages: a DFT investigation.". *Results in Chemistry*, 9:101659, 2024. DOI: https://doi.org/10.1016/j.rechem.2024.101659.

[44] M. J. Saadh, M. Mirzaei, Z. S. Ghnim, R. A. Kareem, S. K. Mohammed, M. Mohany, and S. Ghotekar. "Computer-aided fabrication of an iron-tip enhanced nanocone for providing a smart carrier of Cycloserine (Seromycin) drug through a potential delivery process. ". *Materials Chemistry and Physics*, 338:130646, 2025. DOI: https://doi.org/10.1016/j.matchemphys.2025.130646.